

Nuclear Magnetic Resonance in Cubic Equiatomic Group-VIII Aluminides*

J. J. SPOKAS,† C. H. SOWERS, AND D. O. VAN OSTENBURG‡
Argonne National Laboratory, Argonne, Illinois 60439

AND

H. G. HOEVE
Northern Illinois University, DeKalb, Illinois 60115
 (Received 20 October 1969)

Nuclear-magnetic-resonance measurements are reported for the seven cubic equiatomic group-VIII aluminides: FeAl, RuAl, OsAl, CoAl, RhAl, IrAl, and NiAl. The Al^{27} resonance was studied in each compound and that of Co^{59} in CoAl. The Knight shift, nuclear spin-lattice relaxation rate, linewidth, and intensity were determined at temperatures in the range 4.2–300°K and at 8 and 12 MHz. Except for FeAl, the Al^{27} shifts are much less in magnitude than that of pure Al, and the spin-lattice relaxation times T_1 are 10 to 500 times greater than that of pure Al. T_1T is relatively constant around room temperature, but in each case decreases below about 77°K. An exceptional behavior is observed for Al^{27} in CoAl, where there is an additional contribution to the relaxation rate independent of temperature from 4.2 to 300°K. This is believed to be due to the presence of localized magnetic moments. In every case the linewidth exceeds the theoretical nuclear dipolar width and, while intensity measurements indicate that all transitions of all nuclei contribute to the observed signals, there is distinct evidence of quadrupolar effects. The Knight-shift and T_1 results imply that the s character of the conduction electrons is small at Al sites. This is shown to be in accord with the Engel-Brewer model of intermediate phases in alloy systems.

I. INTRODUCTION

A WEALTH of information concerning the electronic structure of metals and alloys can be derived from NMR observations.¹ Conduction electrons are an important source of internal magnetic fields which cause a shift in the frequency for nuclear magnetic resonance for a given external field. They also contribute to a distribution of resonance frequencies in the sample. Further, the conduction electrons provide an efficient thermal relaxation mechanism for the nuclear spins. The conduction electron relaxation mechanism is usually dominant in metals and alloys.

The group-VIII aluminides are particularly amenable to a NMR study for two reasons. First, aluminum occurs naturally as a single isotope possessing a large gyromagnetic ratio, $\gamma = 2\pi \times 1109.4$ (sec Oe)⁻¹.² Second, most of the equiatomic group-VIII aluminides studied in this work crystallize in the cubic CsCl structure and complications due to quadrupolar couplings are minimized. PdAl and PtAl crystallize in the C face-centered monoclinic and Fe silicide structure, respectively, and their results will be reported elsewhere.

Several NMR studies of NiAl,^{3–6} FeAl, and CoAl

have been reported.^{6–9} The previous studies were concerned primarily with shifts, linewidths and intensities and deviations from exact stoichiometry on these quantities. In one previous study, West⁸ determined the Al^{27} nuclear spin-lattice relaxation times from the saturation characteristics of the cw resonance signals.

The current work represents the following extensions of the previous studies: (a) Inclusion of the additional group-VIII aluminides with the CsCl structure, namely, RuAl, OsAl, RhAl, and IrAl. (b) Direct measurement of the nuclear spin-lattice relaxation time T_1 . (c) Measurement of the magnetic susceptibility of OsAl and IrAl. Except for minor disagreements in the case of CoAl, the present measured shifts agree with those previously reported. The results for the additional compounds studied resemble those for FeAl, CoAl, and NiAl. In particular, RuAl and OsAl have negative shifts, like FeAl, whereas RhAl and IrAl have small positive shifts like CoAl.

The Al^{27} relaxation times determined in the present work are only slightly longer than those previously reported⁸ for FeAl but are significantly greater for NiAl and CoAl. Except for FeAl the T_1 's for Al^{27} are in the range of 15 to 600 times greater than the T_1 of pure Al metal at the same temperature. The relatively weak Al^{27} thermal relaxation is probably due to a small s -conduction-electron density at the Al sites. It is found that T_1T is approximately constant from room temperature to 77°K for each compound, indicating that the predominant relaxation mechanism is through conduction electrons. However, at 4.2°K, T_1T is about a factor of 2 lower than the higher-temperature value. Thus, at

* Work supported by the U. S. Atomic Energy Commission.

† Permanent address: St. Procopius College, Lisle, Ill. 60532.

‡ Present address: De Paul University, Chicago, Ill. 60614.

¹ W. D. Knight, in *Solid State Physics*, edited by F. Seitz and D. Turnbull, (Academic Press Inc., New York, 1956), Vol. 2, p. 93; T. J. Rowland, in *Progress in Materials Science*, edited by B. Chalmers (Pergamon Press, Inc., New York, 1961), Vol. 9.

² G. E. Pake, in *Solid State Physics*, edited by F. Seitz and D. Turnbull (Academic Press Inc., New York, 1956), Vol. 2, Table I, p. 3.

³ J. A. Seitchik and R. H. Walmsley, *Phys. Rev.* **131**, 1473 (1963).

⁴ K. Miyatani, S. Ehara, T. Sato, and Y. Tomono, *J. Phys. Soc. Japan* **18**, 1345 (1963).

⁵ L. E. Drain and G. W. West, *Phil. Mag.* **12**, 1061 (1965).

⁶ G. W. West, *Phil. Mag.* **9**, 979 (1964).

⁷ J. A. Seitchik and R. H. Walmsley, *Phys. Rev.* **137**, A143 (1965).

⁸ G. W. West, *Phil. Mag.* **15**, 855 (1967).

⁹ K. Miyatani and S. Iida, *J. Phys. Soc. Japan* **25**, 1008 (1968).

low temperatures there appear to be additional mechanisms contributing to the relaxation.

In some cases this may be related to the formation of localized magnetic moments. Recently, Caskey and Sellmyer¹⁰ measured the transport properties of CoAl alloys and reported resistivity minima between 23 and 65°K for Co concentrations between 50.4 and 51.5 at.%. The unique temperature dependence of T_1 for Al²⁷ is an independent manifestation of the presence of localized magnetic moments.¹¹ A similar behavior has been found in the galvanomagnetic properties of NiAl.¹²

Neutron diffraction measurements of OsAl reveal no major phase change or ordering and no change in lattice parameters in the temperature range from 77 to 5°K. The systems are metallic with a positive temperature coefficient of resistivity. At room temperature the resistivity of OsAl is 19 $\mu\Omega$ cm. In the current analysis the relaxation rate at room temperature is used as indicative of normal conduction-electron properties.

The linewidths exceed the theoretical dipolar value and below 77°K generally exhibit a slight increase with decreasing temperature. The spin-echo technique used in the present work permits the clarification of the relative importance in the additional width of quadrupolar interactions and Knight-shift inhomogeneities. A preliminary report of this work has been given previously.¹³

II. EXPERIMENTAL METHODS

A. Sample Preparation

The compounds were made from the pure elements by alloying the constituents in an arc furnace. The samples were homogenized in an argon atmosphere at 1000 to 1100°C for 3 to 5 days, and pulverized with a tungsten carbide mortar and pestle. Only the particles passing through a 325-mesh sieve were used for the NMR measurements. The powders were annealed at 900°C for approximately 24 h to remove strains which may have been introduced in the pulverizing process. Some NMR measurements were made on a few samples before annealing and the results are noted below.

B. NMR Techniques

All the spin-lattice relaxation times, signal intensities and some of the Knight shifts were made with a coherent crossed-coil spin-echo spectrometer. It was operated at

either 8 or 12 MHz and employed phase-sensitive detection. The T_1 's were determined using a two-pulse sequence consisting of a 180° pulse followed a time τ later by a 90° pulse. The amplitude of the induction signal following the second pulse was usually found to vary exponentially with τ . Spin-lattice relaxation times T_1 were then determined by fitting the amplitude A versus τ to the equation

$$A = A_0 e^{-\tau/T_1}, \quad (1)$$

where A_0 is a constant. In a few instances the relaxation curves were not simple exponentials. However, a reasonable exponential fit could be made for the greatest pulse spacing from which the T_1 's were then derived.

Knight shifts K at 77°K and below were determined with the spin-echo spectrometer using the signal from Al metal powder as a reference and its known shift $K_{Al} = 0.161\%$ and γ .² The shifts and widths were also determined at room temperature and at 128°K using a Varian Associates wide-line spectrometer. An AlCl₃ solution provided the reference signal for the cw Knight-shift measurements.

Signal intensities were determined from the amplitude of the free-induction signal immediately following a single 90° pulse. Blocking of the rf amplifier prevented observation of the induction signals for 5 to 15 msec after the exciting pulse. A linear extrapolation of the observed free-induction decay was used to obtain its initial amplitude.

To obtain an absolute measure of the intensity, the free-induction decay amplitude of the sample was compared with that of a known reference at the same temperature and with the spectrometer operating at the same frequency. The sample and reference were suspended from a single quartz rod and could be positioned in the crossed coil head from outside the cryostat. In making the signal comparisons, the rf gain was maintained constant.

A 90° pulse nutates the entire nuclear magnetization of the resonant species in the sample, with gyromagnetic ratio γ , into a plane perpendicular to the applied constant field H_0 where it precesses at angular frequency $\omega_0 = \gamma H_0$. This precessing macroscopic nuclear moment M induces a rf voltage in the receiver coil at the precessional frequency ω_0 . The amplitude of the induced voltage V is given by

$$V = 4\pi M \omega_0 n \eta, \quad (2)$$

where n is the pitch of the solenoidal receiver coil and η is a numerical factor taking into account the disposition of the sample relative to the coil. For a sample, whose volume is small in comparison to the coil, and located near the center of the coil η is unity. At the temperatures used in these experiments the nuclear susceptibility χ_N should follow Curie's law so that

$$M = \chi_N H_0 = [\gamma^2 I(I+1)/3kT] H_0 N, \quad (3)$$

¹⁰ G. R. Caskey and D. J. Sellmyer, Fourteenth Annual Conference on Magnetism and Magnetic Materials, New York, 1968 (unpublished).

¹¹ D. O. Van Ostenburg, J. J. Spokas, C. H. Sowers, and H. G. Hoeve, Phys. Letters **30A**, 130 (1969).

¹² Y. Yamaguchi and J. O. Brittain, Phys. Rev. Letters **21**, 1447 (1968).

¹³ D. O. Van Ostenburg, J. J. Spokas, and C. H. Sowers, Bull. Am. Phys. Soc. **11**, 219 (1966); J. J. Spokas, C. H. Sowers, and D. O. Van Ostenburg, *ibid.* **11**, 482 (1966).

where I is the nuclear spin, N is the number of nuclei in the sample, k is Boltzmann's constant, and T is the absolute temperature.

Combining Eqs. (2) and (3) with the condition for resonance, $\omega_0 = \gamma H_0$, the induced voltage under conditions of fixed temperature and frequency is given by

$$V \sim \gamma I(I+1)N\eta. \quad (4)$$

The absolute intensity measurements are based on (4). Each factor on the right-hand side is either known or can be measured for both the sample and the reference. N is directly proportional to the mass. The variation of η with sample volume is determined for a particular coil in a separate experiment. For the measurements reported here $\eta \geq 0.90$. The consistency of (4) was checked by comparing the induction signals from Al^{27} in the pure metal, Na^{23} in NaCl crystals, and H^2 in water. Within the accuracy of the measurements, (4) accounted for the relative signal strengths.

III. EXPERIMENTAL RESULTS

A. Knight Shift

Results of the Knight-shift measurements are summarized in Table I. It is noted that with the exception of FeAl the magnitude of the shifts are relatively small. Compounds of Fe , Ru , and Os , which appear in the same column of the Periodic Table, have negative shifts whereas the others are positive. The FeAl , CoAl , and NiAl shifts are in substantial agreement with previous measurements.³⁻⁹ The Knight-shift behavior shown by the compounds of the first transition series is also shown by the compounds of the second and third series. In each series, the Knight shift is first negative and progressively becomes more positive with increasing atomic number.

B. Spin-Lattice Relaxation

The spin-lattice relaxation times are presented in Fig. 1, where the product T_1T is plotted on a semilog scale as a function of T . The semilog scale was chosen to better accommodate the whole range of values rather than to display a particular temperature dependence. The values range from about 2.0 sec °K in FeAl to 1000 sec °K found in IrAl . For comparison, $T_1T = 1.81$ sec °K¹⁴ in pure Al metal.

TABLE I. Al^{27} Knight shifts (%) at 300 and 128°K for the CsCl group-VIII aluminum compounds.

Compound	300°K	128°K
FeAl	-0.400	-0.343
RuAl	-0.033	-0.043
OsAl	-0.023	-0.037
CoAl	0.013	0.012
RhAl	0.037	0.039
IrAl	0.019	0.019
NiAl	0.055	0.057

¹⁴ J. J. Spokas and C. P. Slichter, Phys. Rev. **113**, 1462 (1959).

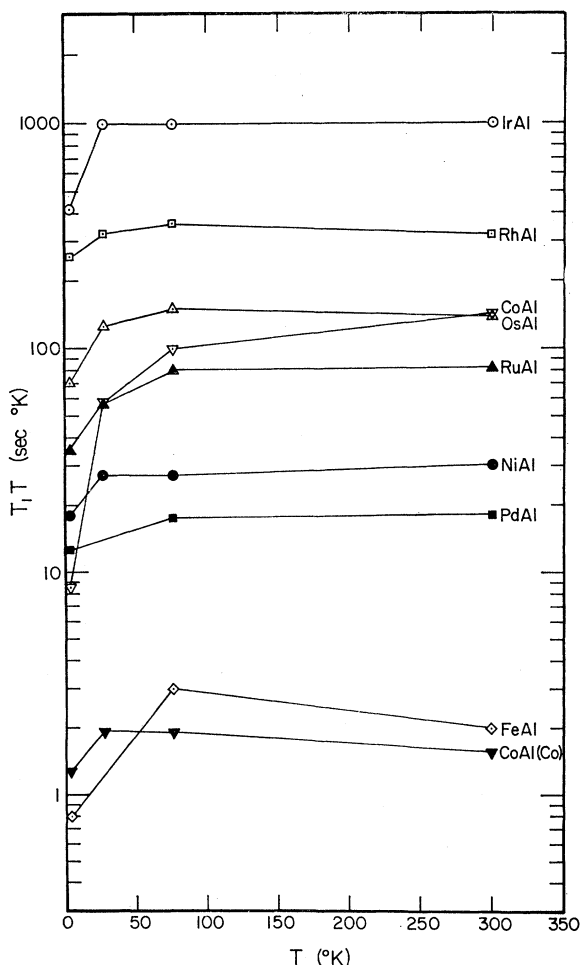


FIG. 1. T_1T for Al^{27} in the group-VIII aluminides plotted on a logarithmic scale versus absolute temperature. The Co^{60} data in CoAl are labeled $\text{CoAl}(\text{Co})$.

Besides the wide range of values found for these compounds there is another conspicuous feature of the T_1 results, namely, T_1T is not completely independent of T . The strongest temperature dependence is observed at the lower temperatures. T_1T is nearly constant above 77°K, where CoAl and FeAl show the only significant variation (about 50%).

The Al^{27} relaxation in CoAl is represented as a function of temperature by

$$1/T_1T = A + B/T, \quad (5)$$

where $A = 0.005$ sec °K⁻¹ and $B = 0.35$ sec⁻¹. This expression is similar to that recently derived by Giovannini and Heeger¹⁵ for relaxation in the presence of a localized magnetic moment. This process involves a virtual excitation and relaxation of the localized moment via the conduction electrons. The magnitude

¹⁵ B. Giovannini and A. J. Heeger, Solid State Commun. **7**, 287 (1969).

of the s - d exchange integral J estimated for this system is about 10 eV.¹¹

The relaxation rate for Co⁵⁹ in CoAl is more than 300 times that of Al²⁷ and is probably dominated by an orbital contribution at the Co sites. Its temperature dependence is of the Korringa type except at temperatures below 25°K. The T_1 for Co⁵⁹ probably also contains a contribution from the local moment; however, this is probably masked by the much greater orbital term. The 60% intensity of the Co⁵⁹ signal indicates that the localized moments do not exist at all Co sites.

In several instances, but only at temperatures of 27°K and below, the longitudinal relaxation curves were not simple exponentials. The most severe departures from simple exponential relaxation were found in RuAl and OsAl at 4.2°K. The relaxation curves at 4.2°K in two independently prepared unannealed RuAl powders could be represented by a sum of two exponentials, one of time constant 8.5 sec representing approximately 75% of the initial amplitude and the other of time constant approximately 1.5 sec. After one of these powders was given a prolonged anneal, it yielded a more pronounced complex decay, which again could be well represented by a sum of two exponentials with nearly equal intensity and time constants of 11.7 and 2.0 sec. Although there were attendant changes in the Bloch decay shape, the extrapolated initial intensities of the induction signals before and after annealing indicated approximately 100% intensity.

In OsAl, also, the relaxation curves at 4.2°K were affected by annealing the powders. In this case there are two important facts: (a) The relaxation curve in unannealed powder was a simple exponential with a time constant of 16 sec. (b) In the annealed powder the curve could be decomposed into two exponentials with time constants of 9 sec and approximately 1 sec. The former represents about 70% of the initial amplitude. The result of annealing is thus opposite in RuAl and OsAl. In OsAl the time constants are reduced, whereas in RuAl they are increased. Annealing effects, not as pronounced, can also be found in the other compounds. However, the high-temperature relaxation is always exponential and essentially invariant with respect to preparation method and annealing treatment. For these reasons the constant values found at high temperature are regarded as intrinsic and are discussed theoretically in Sec. IV.

C. Linewidth and Intensity

The room-temperature linewidths determined by cw measurements are summarized in Table II. Theoretical linewidths and the lattice constant a derived from x-ray diffraction patterns are also given in the table. The theoretical widths are based on Van Vleck's expression for the nuclear dipolar second moment,¹⁶

$$\Delta H_2^2 = (3/5)I(I+1)\gamma^2\hbar^2 \sum_j r_{0j}^{-6} + (4/15)\sum_f I_f(I_f+1)\gamma_f^2\hbar^2 r_{0f}^{-6}, \quad (6)$$

where j and f refer to like and unlike nuclei, respectively. Values for the CsCl lattice sums,

$$\sum_j r_{0j}^{-6} = 8.40/a^6 \quad \text{and} \quad \sum_f r_{0f}^{-6} = 20.65/a^6, \quad (7)$$

were taken from Gutowsky and McGarvey.¹⁷ The contribution to the linewidth of like and unlike nuclei are shown separately in Table II. Twice the square root of the sum is taken as the theoretical linewidth. This would be the full width between points of maximum slope for a Gaussian shape and is expected to correlate closely with the widths measured between points of maximum slope of the observed absorption lines.

The observed width exceeds the theoretical width in each case. The discrepancy is less than a factor of 2 except for the Al²⁷ resonance in CoAl, where it is approximately 2.0. Among the group-VIII aluminides, several different mechanisms are responsible for the excess linewidth. Spin-echo measurements enabled a partial identification of the excess width as described below.

The free-induction decay following a suitably long and intense rf pulse at the Larmor frequency is the Fourier transform of the absorption line.¹⁸ Thus the Bloch decay provides an independent and distinct view of the NMR absorption line. Observed T_2^* 's of the Bloch decays at room temperature and 4.2°K are summarized in Table III. The observed T_2^* 's were taken as the time required for the induction signal to drop to e^{-1} of its initial value. Calculated decay times were obtained from the theoretical linewidths given in Table II according to the equation

$$T_2^* = (\gamma\Delta H_{rms})^{-1}. \quad (8)$$

Equation (8) was chosen because it is precise for a Gaussian absorption line.

The Bloch decay shapes are not the same for all samples. The shapes vary from nearly Gaussian, nearly exponential, to several that are a sum of two decays having time constants differing by factors of 2 to 3. One must therefore exercise some caution in comparing the T_2^* values of different compounds or even of the same compound at different temperatures. Also, annealing usually produces a change in shape of the Bloch decay.

Bloch decays which are a composite of two or more contributions with quite different characteristic times are most likely examples of secular first-order quad-

¹⁷ H. S. Gutowsky and B. R. McGarvey, *J. Chem. Phys.* **20**, 1472 (1952).

¹⁸ A. Abragam, *The Principles of Nuclear Magnetism* (Oxford University Press, Oxford, England, 1961), p. 114.

¹⁶ J. H. Van Vleck, *Phys. Rev.* **74**, 1168 (1948).

TABLE II. Calculated and observed cw linewidths. The calculated second moments are based upon nuclear dipolar coupling alone. Twice the calculated rms width is also listed as this quantity is equal to the peak-to-peak derivative width ΔH_{ms} for a Gaussian shape. The last column lists the experimentally observed widths measured between points of maximum slope.

Compound ^c	Lattice constant ^a (10^{-8} cm)	Calculated from like nuclei (ΔH^2) (Oe ²)	Calculated from unlike nuclei (ΔH^2) (Oe ²)	Total (ΔH^2) (Oe ²)	$2(\Delta H_{rms})_{theoret}$ (Oe)	$(\Delta H_{ms})_{obs}$ ^b (Oe)
<i>FeAl</i>	2.908	3.94	<0.005	3.94	3.97	6.7
<i>RuAl</i>	2.950	3.65	0.04	3.69	3.84	5.8
<i>OsAl</i>	3.005	3.29	0.02	3.31	3.64	5.4
<i>CoAl</i>	2.862	4.33	7.07	11.40	6.75	14.0
<i>RhAl</i>	2.990	3.25	<0.005	3.25	3.61	4.9
<i>IrAl</i>	2.980	3.38	0.009	3.39	3.68	5.5
<i>NiAl</i>	2.887	4.11	<0.005	4.11	4.05	5.3
<i>CoAl</i>	2.862	6.46	4.73	11.19	6.69	11.5
<i>OsAl</i>	3.005	0.02	3.59	3.61	3.80	...
<i>NiAl</i>	2.887	0.0026	4.49	4.49	4.24	4.9 ^d

^a W. B. Pearson, *A Handbook of Lattice Spacings and Structures of Metals and Alloys* (Pergamon Press, New York, 1958), Vols. 1 and 2.

^b Measurements were made at 300°K and 12 MHz.

^c The entries pertain to the italicized element in the compound formula.

^d Reference 5.

rupole broadening. IrAl is the most striking example. It shows a fast component with a time constant of 20 times less than the persistent component. The fast component in IrAl decays nearly entirely within the deadtime of the receiver. The quadrupole nature of the broadening was confirmed by the observation that a 180° pulse within the time T_2^* after a 90° pulse produced no refocusing of the transverse nuclear magnetization. A rephasing due to inhomogeneous magnetic broadening such as found in a Knight-shift inhomogeneity or with external magnetic field gradients would of course be refocused by the 180° pulse. At the same time a pulse producing an approximately 40° nutation gave a prominent echo. Solomon¹⁹ has theoretically shown that for $I = \frac{5}{2}$, a 40° pulse following one of 90° will yield the maximum refocusing of the dephasing caused by first-order quadrupole interactions.

The largest linewidth is observed for Al²⁷ in CoAl. The evidence¹¹ for the existence of localized magnetic moments in this compound implies that the linewidth should broaden at low temperatures. The width can be separated into two terms δH_0 and $\delta H(T)$, where only the latter is temperature-dependent. The sample used in this investigation contains an excess of about 0.5-at.% Co. Miyatani and Iida⁹ investigated a CoAl compound containing 0.4-at.% excess Co which is close in composition to the sample used in the current work. For this sample they find that the magnetic susceptibility obeys Curie's law with a Curie constant of about 2×10^{-3} emu °K/g. Furthermore, $\delta H(T)$ can be divided into two parts²⁰: (i) δH^{dip} arising from the magnetic dipolar interaction, and (ii) δH^{ex} arising from the Ruderman-Kittel-Kasuya-Yosida (RKKY)²¹ interaction. Each interaction represents a coupling between the Al nuclei and the localized magnetic

moment complex. Gossard *et al.*²² have shown that under certain approximations, $\delta H^{ex} = \text{const} \times \delta H^{dip}$. Since δH^{dip} is proportional to the concentration of magnetic impurities and the thermal average $\bar{\mu}_z$ of the localized magnetic moment complex, $\delta H(T) \propto T^{-1}$. A graph of the linewidth versus T^{-1} gives $\delta H_0 \approx 14$ Oe. Thus, the temperature-dependent part of the linewidth is small. At room temperature, it is completely masked by the temperature-independent contribution. At 4.2°K it contributes about 20% to the total width. This value is not inconsistent with $J = 10$ eV¹¹ if $\delta H^{dip} \approx 1$ Oe. Miyatani and Iida quote values of $\delta H^{dip} \approx 4-6$ Oe at 77°K; however, these estimates were based on samples containing larger amounts of Co.

A quadrupole echo was observed in all samples before and after annealing. However, in CoAl there is evidence of inhomogeneous magnetic broadening as confirmed by the occurrence of a 90°–180° echo. In FeAl and NiAl at room temperature such an echo was not found, although in FeAl at 4.2°K it was very prominent.

The quadrupole echo lifetime in FeAl was approximately 220 μsec , at room temperature and approx-

TABLE III. Comparison of measured and calculated Bloch decay lifetimes. The last column lists the observed Bloch decay amplitudes determined as described in Sec. II B.

Sample ^a	Calc	T_2^* (μsec)		Induction amplitude (%)
		Observed 300°K	Observed 4.2°K	
<i>FeAl</i>	72.3	25±3	4.1±0.5	40
<i>RuAl</i>	74.7		67.0±0.6	75
<i>OsAl</i>	78.8	42±4	36.0±4	100
<i>CoAl</i>	38.3	19±1	14.5±1	100
<i>RhAl</i>	79.7	64±6	56.0±5	80
<i>IrAl</i>	77.9	65±6	64.0±6	50
<i>NiAl</i>	70.8	39±4	27.0±3	100
<i>CoAl</i>	47.3	18±2	8.5±1	60

^a Values listed in the table pertain to the italicized element.

¹⁹ I. Solomon, Phys. Rev. **110**, 61 (1958).

²⁰ R. E. Behringer, J. Phys. Chem. Solids **2**, 209 (1957).

²¹ M. A. Ruderman and C. Kittel, Phys. Rev. **96**, 99 (1954); T. Kasuya, Progr. Theoret. Phys. (Kyoto) **16**, 45 (1956); K. Yosida, Phys. Rev. **106**, 893 (1957).

²² A. C. Gossard, V. Jaccarino, and J. H. Wernick, J. Phys. Soc. Japan Suppl. **17**, 88 (1962).

imately 350 μsec at 4.2°K. The 90°–180° echo lifetime at 4.2°K is approximately 90 μsec which implies a narrower absorption line than expected for nuclear dipolar coupling alone. The increased echo lifetimes are manifestations of partial suppression of spin-spin processes by static quadrupole and magnetic couplings.

The last column in Table III gives the signal intensity determined as described in Sec. II. It is seen that for the most part, all nuclei in the sample contributed fully, or nearly so, to the observed signal. In the case of IrAl, it seems clear that the reduced intensity is due entirely to the existence of a sizable first-order quadrupole broadening. As a result, there is an appreciable fast component in the Bloch decay, as mentioned above, which is largely obscured by the deadtime of the amplifier. The situation is not as clear for Al²⁷ in FeAl and Co⁵⁹ in CoAl, which also show significant losses of intensity. Here the wipeout could be due to a combination of paramagnetic clusters, localized magnetic moments, and large electric field gradients around defects.

D. Magnetic Susceptibility

The temperature dependence of the magnetic susceptibilities of OsAl and IrAl was investigated at 4.2, 77°K, and room temperature using a Faraday method. The measurements were made with Mohr's salt as a reference. The maximum magnetic field used was 7 kOe. No indication of a ferromagnetic component was observed.

The current results are shown in Fig. 2 and compared with values previously reported for Al,²³ NiAl,^{9,24} RhAl,²⁴ FeAl, and CoAl.^{8,9}

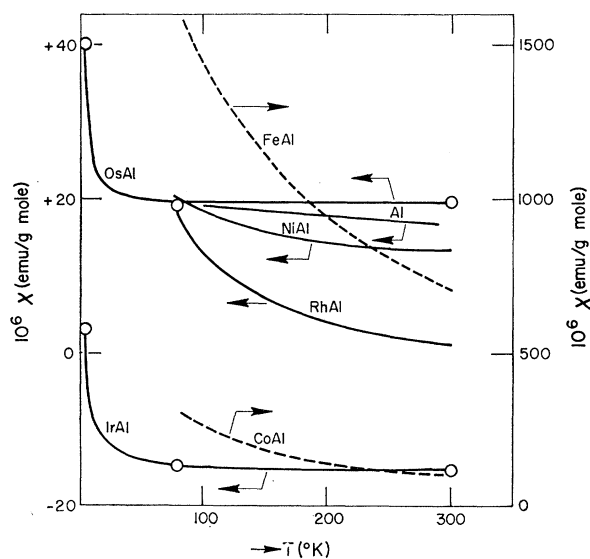


FIG. 2. Temperature dependence of the magnetic susceptibilities in emu per g mole $X_{0.5}\text{Al}_{0.5}$. The arrows indicate which scale is to be used.

²³ M. A. Taylor, *J. Phys. Radium* **20**, 829 (1959).

²⁴ M. Höhl, *Ann. Phys. (Paris)* **19**, 15 (1967).

Somewhere below 77°K the susceptibilities exhibit a temperature dependence different from that at higher temperatures. This may be related to the anomalous temperature-dependent behavior of the relaxation rate below 77°K.

IV. DISCUSSION

Many physical and electronic properties of metals and alloys can be explained in terms of theories based upon the band concepts of solids.²⁵ However, these theories have not yet been able to predict the various types of crystal structures which are stable for the pure metals and their alloys. The most successful model in this respect is based upon the original ideas of Engel²⁶ and more recently extended by Brewer.²⁷ The essence of the Engle model is as follows: The occurrence of the bcc structure, the hcp structure, and the fcc structure is ascribed to concentrations of one, two, and three valence electrons per atom, respectively, with these valence electrons in the *s* or *p* state. For the transition metals, all unpaired *d* electrons take part in the bonding, but they do not play a role in controlling the type of crystal structure. This is determined only by the number of *s* and *p* electrons. In general, the process of forming a particular metallic crystal structure from the isolated atoms is comprised of two steps: (a) an excitation process, involving a promotion energy, in which an atom is excited from its ground state to an excited state containing the required number of *s* and *p* electrons to form the known crystal structure; (b) a condensation process, involving a bonding energy, in which the atoms from the gaseous state condense to form the crystal. The final electronic configuration is, consequently, determined by two opposing factors since an increase in the promotion energy may allow more electrons for bonding and thus cause an increase in the bonding energy, which can more than offset an increase in the former. These ideas have been independently confirmed through thermodynamic calculations of Brewer.²⁷ In this paper, concern is not for the prediction of a particular crystal phase, but rather the electronic configurations of the atoms in the compounds, the amount of charge transferred between the atoms, and how this is related to the observed Knight shifts and relaxation times.

Since the compounds are equiatomic and Al has no *d* electrons, the replacement of a transition-metal atom by one of Al will destroy all of the *d* bonding that originally existed between the transition-metal atoms and their nearest neighbors. Under these conditions it is believed

²⁵ N. F. Mott and H. Jones, *The Theory of the Properties of Metals and Alloys* (Dover Publications, Inc., New York, 1958).

²⁶ N. Engel, *Kem. Maanesblad*, No. 5 (1949); No. 6 (1949); No. 8 (1949); No. 9 (1949); No. 10 (1949).

²⁷ L. Brewer, University of California Lawrence Radiation Laboratory Report No. UCRL-10701, 1964 (unpublished); in *High Strength Materials*, edited by V. F. Zackey (John Wiley & Sons, New York, 1965); in *Phase Stability in Metals and Alloys*, edited by P. S. Rudman *et al.* (McGraw-Hill Book Co., New York, 1966).

TABLE IV. Electron configurations of the metals and compounds according to the Engel-Brewer correlation. The notation (s,p) refers to a common conduction band formed from the transition and Al metal s and p valence states.

Element	Configuration		Crystal structure	Compound	Configuration	Crystal structure
	Ground state	Metallic state				
Al	$(3s)^2(3p)^1$	$(3s)^1(3p)^2$	fcc			
Fe	$(3d)^6(4s)^2$	$(3d)^7(4s)^1$	bcc	FeAl ^a	$(3d)^{8.6}(s,p)^{1.2}$	CsCl
Co	$(3d)^7(4s)^2$	$(3d)^7(4s)^1(4p)^1$	hcp	CoAl ^a	$(3d)^{9.2}(s,p)^{1.4}$	CsCl
Ni	$(3d)^8(4s)^2$	$(3d)^7(4s)^1(4p)^2$	fcc	NiAl ^a	$(3d)^{10}(s,p)^{1.5}$	CsCl
Ru	$(4d)^7(5s)^1$	$(4d)^6(5s)^1(5p)^1$	hcp	RuAl	$(4d)^9(s,p)^1$	CsCl
Rh	$(4d)^8(5s)^1$	$(4d)^6(5s)^1(5p)^2$	fcc	RhAl	$(4d)^{10}(s,p)^1$	CsCl
Pd	$(4d)^{10}(5s)^0$	$(4d)^7(5s)^1(5p)^2$	fcc	PdAl	...	C face-centered monoclinic
Os	$(5d)^6(6s)^2$	$(5d)^6(6s)^1(6p)^1$	hcp	OsAl	$(5d)^9(s,p)^1$	CsCl
Ir	$(5d)^7(6s)^2$	$(5d)^6(6s)^1(6p)^2$	fcc	IrAl	$(5d)^{10}(s,p)^1$	CsCl
Pt	$(5d)^9(6s)^1$	$(5d)^7(6s)^1(6p)^2$	fcc	PtAl	...	FeSi

^a The nonintegral configurations were obtained from L. Brewer (private communication).

that the structure with the fewest unpaired d electrons will be favored.²⁸ Consequently, for these compounds a maximum number of electrons is transferred from Al to the transition-metal d band, retaining the required amount of s and p electrons to form the bcc or in this case the CsCl structure. Table IV gives the electronic configurations of the pure metals and compounds according to the Engel-Brewer correlation. The resulting number of s and p electrons required to form the CsCl structure ranges from 1 to 1.5²⁹ and is found by averaging over an Al and transition-metal atom pair. Since the d electrons are localized,³⁰ they do not play a part in this averaging process. Table IV gives the number of conduction electrons per atom for each compound. These values are used in the calculations below.

There are additional reasons why these compounds are believed to be of the charge-transfer type. For example, RuAl and OsAl have a silver and pinkish-gold color, respectively. This is suggestive of a charge transfer from Al to the transition-metals Ru and Os resulting in electronic configurations with optical properties similar to those of silver and gold, respectively.³¹ Also, relative to pure Al metal, the Knight shift is very small and the nuclear spin-lattice relaxation time long.

For ordinary metals the Fermi contact interaction is usually the dominant coupling between the nuclear moments and the conduction electrons. For this mechanism the Knight shift is expressed in the form¹

$$K = (8/3)\pi\beta^2 n(E_F)\Omega\langle|\psi(0)|^2\rangle_{av}, \quad (9)$$

where β is the Bohr magneton, $n(E_F)$ the bare density

of states evaluated at the Fermi level, $\psi(0)$ is the value at the nucleus of the s -wave function normalized over the atomic volume Ω , and $\langle|\psi(0)|^2\rangle_{av}$ is the average of the square of $\psi(0)$ taken over all electronic states on the Fermi surface. Through the Korringa³² relation (non-interacting electrons), the Knight shift and nuclear spin-lattice relaxation time are related by

$$T_1TK^2 = 2\beta^2/kh\gamma^2 \equiv S, \quad (10)$$

where k and h are Boltzmann's and Planck's constant, respectively. This equation shows that a small K implies a large T_1 . Generally these compounds show this behavior. From Eq. (9) a small magnitude for the Al²⁷ Knight shift implies either a small density of states at the Fermi surface or a small amount of s -electron density remaining at the Al site. It will be shown that the latter implication is the best suited to describe the results of this investigation.

Applying Eq. (9) to the Al²⁷ shift in the XAl compounds yields

$$K_{Al/XAl} = (8/3)\pi\beta^2 [n(E_F)]_{XAl} \xi_{Al/XAl} |\psi_{Al}(0)|^2, \quad (11)$$

where

$$\xi_{Al/XAl} \equiv \frac{\langle|\psi_{Al/XAl}(0)|^2\rangle_{av}}{|\psi_{Al}(0)|^2}.$$

$|\psi_{Al}(0)|^2$ is the $3s$ -electron density at the nucleus of a free Al atom. Of course, both the wave functions for the free atom as well as that for the compound are normalized over the volume of the respective atoms. The factor $\xi_{Al/XAl}$ allows a comparison of the wave functions in the various compounds from measured shifts and densities of states. The density of states is usually determined from the measured low-temperature specific-heat coefficient. Unfortunately such determinations have only been made for NiAl and FeAl among the group-VIII aluminides. In order to make this comparison on a uniform basis for all the compounds, theoret-

³² J. Korringa, *Physica* **16**, 601 (1950).

²⁸ W. Hume-Rothery, *Progress in Material Science*, edited by B. Chalmers *et al.* (Pergamon Press, Inc., New York, 1967), p. 257.

²⁹ Reference 28, p. 248.

³⁰ J. H. Wood, *Phys. Rev.* **117**, 714 (1960).

³¹ A. Magneli, L. E. Edshammar, T. Dagerhamn, and S. Westman, University of Stockholm, Stockholm, Sweden, Report No. AD 452640, 1964 (unpublished).

ical values of $n(E_F)$ based on the free-electron model and the band occupation numbers given in Table IV were used.

Another difficulty in applying Eq. (11) arises from the fact that the measured shifts are not due exclusively to the Fermi contact interaction. There is no clear procedure for separating from the measured shift the contribution due to just the contact interaction. The fact that some shifts are negative is conclusive evidence of the importance of additional shift mechanisms. Further, since the separate shift contributions may be both positive and negative, the observed shift is not a reliable upper or lower bound for the contact contribution.

This uncertainty can be avoided by referring to the measured relaxation rate T_1^{-1} . If several independent mechanisms contribute to the rate, the observed rate is the sum of the separate contributions which are all positive. Therefore, the contact interaction produces a rate which cannot be larger than that observed. Thus, a more meaningful comparison of the wave functions in the compounds can be made. The procedure is to solve Eq. (10) for K and substitute into Eq. (11). This gives

$$(T_1 T)^{-1/2}_{Al/XAl} = (8/3)\pi (\frac{1}{2}k\hbar)^{1/2} \beta \gamma [n(E_F)]_{XAl} \times \xi_{Al/XAl} |\psi_{Al}(0)|^2. \quad (12)$$

The comparison can be further simplified by taking the ratio of Eq. (12) applied to one of the compounds and Eq. (12) applied to Al metal. Then,

$$P_{T_1} \equiv \frac{\xi_{Al/XAl}}{\xi_{Al/Al}} = \frac{(T_1 T)^{1/2}_{Al/Al} [n(E_F)]_{Al}}{(T_1 T)^{1/2}_{Al/XAl} [n(E_F)]_{XAl}}. \quad (13)$$

Now in the free-electron model $n(E_F)$ is proportional to $\rho_{\text{cond}}^{1/3}$, where ρ_{cond} is the volume density of conduction electrons. Values of P_{T_1} computed from Eq. (13) and the measured rates are given in Table V. Except for FeAl and NiAl, the conduction-electron densities at the Al nuclei in the compounds are less than 10% of the free-atom value. In the case of FeAl, there is no doubt a significant core-polarization contribution to the rate which was not subtracted. Consequently, the value of the wave-function density of 0.51 is clearly an overestimate. In the case of NiAl, the listed value may be a true representation of the actual density for the compound.

It is also interesting to compare the NMR derived wave-function density to that expected for completely free conduction electrons. For this comparison, the coefficient η is introduced and defined by

$$\langle |\psi_{Al/XAl}|^2 \rangle_{\text{av}} \equiv \eta_{Al/XAl} (1/\Omega_{XAl}), \quad (14)$$

with Ω_{XAl} the atomic volume in compound XAl. Ratios of η 's for the various compounds with that of Al metal are also listed in Table V. These ratios are a measure of the degree to which the free-electron model is obeyed in the various compounds versus Al metal.

TABLE V. Measures of the conduction electrons remaining at the Al sites in the various compounds relative to pure Al metal.

Compound	P_{T_1}	$\xi_{Al/XAl}^a$	$\eta_{Al/XAl}$
			$\eta_{Al/Al}$
FeAl	1.40	0.51	0.63
RuAl	0.25	0.09	0.14
OsAl	0.18	0.07	0.10
CoAl	0.15	0.05	0.10
RhAl	0.12	0.04	0.07
IrAl	0.07	0.02	0.04
NiAl	0.38(0.28) ^b	0.14(0.10) ^b	0.27

^a $\xi_{Al/Al} = 0.36$ (see Ref. 1).

^b Values in parenthesis were derived using χ_{spin} calculated from low-temperature specific-heat data. For NiAl the value determined from Eq. (13) is in close agreement with that quoted in Ref. 3.

A value of unity implies equal validity of the free-electron model in both the compound and Al metal. The η 's show a similar result to that of the ξ 's, namely, that the wave-function density is far from uniform, and it is particularly low at the Al sites in most of the compounds. As before, FeAl and NiAl show the most significant densities at the Al sites.

These results can be expressed in terms of the tight-binding formalism.³³ In this model the electronic wave function is taken to be of the form

$$\psi_k(\mathbf{r}) = \frac{1}{\sqrt{N}} \sum_{j,m} e^{i\mathbf{k} \cdot \mathbf{R}_m} a_j \phi_j(\mathbf{r} - \mathbf{R}_m), \quad (15)$$

where ϕ_j is the normalized atomic orbital centered on the j th atom of the m th cell. It describes the state of the valence electron in the free atom. N is the number of unit cells, k is the Bloch wave vector, and $\sum_j |a_j|^2 = 1$. In this scheme

$$P_{T_1} = \xi_{Al/XAl} |a_{Al/XAl}|^2 / \xi_{Al/Al}.$$

It is immediately apparent from Table V that there is little s character remaining in the wave function at the Fermi surface at the Al sites. The Al²⁷ Knight shift of those compounds in the Fe column are all negative, and they become positive and progressively larger as one progresses towards increasing atomic number in each period. This is in accord with the complete filling of the d bands in progressing to the right-hand side of the group-VIII elements. It requires fewer electrons to be transferred from Al to fill these partially empty shells. From the sixth column, Table IV, it can be seen that FeAl, RuAl, and OsAl still have an unfilled d shell. This may account for the negative Knight shifts in these compounds through the RKKY mechanism.²¹ Seitchik and Walmsley⁷ attributed the large negative shift in FeAl to this mechanism. On the other hand, Miyatani and Iida⁹ attribute the large negative shift in FeAl to a p band with a high density of states. It is likely that both mechanisms are operative in all of

³³ A. M. Clogston and V. Jaccarino, Phys. Rev. **121**, 1357 (1961).

these compounds. For NiAl, using the measured low-temperature specific-heat data, an experimental value of P_{T_1} can be obtained (Table V, footnote b). The value derived from experiment is about 27% lower than calculated from the free-electron model. This difference is probably due to the fact that $n(E_F)$ values derived from low-temperature specific-heat measurements are enhanced by electron-phonon and possible electron-magnon effects.

The influence of electron-electron interactions have been included into the theory through the Korringa relation by Moriya³⁴ and Narath and Weaver.³⁵ They find that Eq. (10) is modified to

$$K^2 T_1 T = SK(\alpha)^{-1}, \quad (16)$$

where $K(\alpha)$ is a measure of the enhancement due to the spin susceptibility and the nuclear spin-lattice relaxation rate. The parameter α is directly related to the interaction potential. Using Eq. (16) and the values of $K(\alpha)$ versus α from Ref. 35, values of α were derived for those compounds with positive shifts and are listed in the fifth column of Table VI. Except for Al in CoAl and pure Al, α is very large. This implies that these compounds are largely exchange-enhanced and may be one of the contributing factors in the increased relaxation rate below 77°K. A more detailed account of this effect is currently under investigation. The fact that α for Co⁵⁹ and Al²⁷ in CoAl differ, may be primarily due to two effects: (a) The magnetic susceptibility is not uniformly enhanced, and (b) relaxation associated with core-polarization and orbital effects are much more significant for Co than Al. For these compounds (b) is believed the most likely. A correction to the relaxation rate due to electron-electron enhancement effects is precluded since this requires a knowledge of the Fermi surface in these compounds [see Eq. (22) of Ref. 35].

For pure Al, Shyu *et al.*³⁶ have shown that the total core-polarization contribution to the Knight shift is about 8% of the direct one and of the same sign and the orbital part is negligible. Consequently, for pure Al, Eq. (10) can reasonably be used to describe the relaxation rate. On the other hand, for the XAl compounds, the relaxation rate very likely contains con-

TABLE VI. Correlation of Knight shifts and room-temperature spin-lattice relaxation times.

Sample	K (%)	$T_1 T$ (sec °K)	$T_1 T K^2/S$	α
CoAl	+0.013	200	~1	~0
NiAl	+0.055	30	2.3	0.78
RhAl	+0.037	340	12.0	0.97
IrAl	+0.019	1000	9.3	0.96
Al	+0.162	1.81	1.2	0.35
CoAl	+0.545	1.9	12.0	0.97

tributions to the rate associated with p states of the conduction band. In all cases the orbital contribution to K and T_1 at the Al site can be neglected, as this mechanism is localized to a particular site and is known to be small for Al.^{36,37}

Further evidence which supports the charge-transfer model is given by the Knight shift of Ni⁶¹ and Co⁵⁹ in NiAl and CoAl. For Ni⁶¹ in NiAl (50.3% Al), Drain and West⁵ report a positive shift of $0.189 \pm 0.005\%$ relative to nickel carbonyl. This positive shift is in accord with the idea that for NiAl the d band is completely filled. Likewise, the positive and temperature-independent shift of Co⁵⁹ in CoAl confirms the hypothesis for this compound.

V. CONCLUSION

NMR measurements were made on seven cubic equiatomic group-VIII aluminides. The results show that charge is transferred from Al to the transition metal. In CoAl there is evidence for the presence of localized magnetic moments due to an excess of Co over the stoichiometric amount. The general, over-all conclusions are shown to be consistent with the predictions of the Engel-Brewer model of intermediate phases in alloy systems.

ACKNOWLEDGMENTS

The authors wish to thank Dr. A. E. Dwight, Dr. L. V. Azaroff, Dr. J. O. Brittain, and R. A. Connor for supplying the samples. Dr. M. H. Muller made the neutron diffraction measurements and Dr. J. A. Horak determined the resistivity. In particular, we would like to thank Dr. L. Brewer for a critical reading of the manuscript and several helpful discussions.

³⁴ T. Moriya, J. Phys. Soc. Japan **18**, 516 (1963).

³⁵ A. Narath and H. T. Weaver, Phys. Rev. **175**, 373 (1968).

³⁶ W. Shyu, T. P. Das, and G. D. Gaspari, Phys. Rev. **152**, 270 (1966).

³⁷ D. O. Van Ostenburg, D. J. Lam, H. D. Trapp, D. W. Pracht, and T. J. Rowland, Phys. Rev. **135**, A455 (1964).